Cell, Vol. 96, 833–845, March 19, 1999, Copyright ©1999 by Cell Press

Discs Lost, a Novel Multi-PDZ Domain Protein, Establishes and Maintains Epithelial Polarity

Manzoor A. Bhat,*† Shayan Izaddoost,‡ Yue Lu,† Kyung-Ok Cho,‡ Kwang-Wook Choi,‡§ and Hugo J. Bellen*†‡§‖
*Howard Hughes Medical Institute
†Department of Molecular and Human Genetics
‡Department of Cell Biology
§Program in Developmental Biology
Baylor College of Medicine
Houston, Texas 77030

Summary

Polarization of epithelial cells depends on a hierarchical process whereby specific membrane-associated proteins become targeted to specialized membrane domains. Here, we describe a novel *Drosophila* protein, Discs Lost (DLT), that plays a crucial role in the polarization of embryonic epithelia during cellular blastoderm formation. At subsequent stages of development, DLT interacts with the apical determinant Crumbs (CRB) and the laterally localized protein Neurexin IV (NRX IV). Mutations in *dlt* or double-stranded RNA interference lead to aberrant localization of CRB and NRX IV and cause a concomitant loss of epithelial cell polarity. Hence, DLT is required to establish and maintain cell polarity and participates in different molecular complexes that define apical and lateral membrane domains.

Introduction

In most multicellular organisms, epithelial layers are characterized by a pronounced apico–basal polarity. They form the boundaries between different compartments and control the directional flow of molecules. In vertebrates, differentiation of epithelial cells involves the progressive acquisition of complex intercellular junctional structures between lateral membranes (Drubin and Nelson, 1996; Gumbiner, 1996). These structures consist of tight junctions (TJs) and adherens junctions (AJs) spatially organized as a belt at the apical and lateral domain of epithelial cells. TJs are the most apical, bring adjacent plasma membranes in close proximity, prevent transepithelial diffusion, and restrict membrane proteins to their respective domains (Balda and Matter, 1998). AJs form the zonula adherens (ZAs) and participate in cell–cell interactions and intercellular communication (Gumbiner, 1996; Yap et al., 1997).

In *Drosophila*, epithelial polarization becomes apparent during cellularization. Although several genes have been isolated that are required for cellularization, none have been proposed to play a role in establishing cell polarity (Foe et al., 1993; Schejter and Wieschaus, 1993; Tepass, 1997). The hallmarks of polarized cells (i.e., various sophisticated junctional complexes, including the AJs and septate junctions [SJs]) are gradually acquired during development and are not present early after cellularization (Tepass, 1997). Unlike vertebrate cells, AJs form the most apical belt. The SJs are basal to the AJs, are larger in size than the vertebrate TJs, and only appear relatively late in embryogenesis. However, SJs show similarities to TJs, suggesting that they play an equivalent role (Woods and Bryant, 1993; Marfatia et al., 1994; Baumgartner et al., 1996).

Formation of polarized epithelia in most species is dependent on and controlled by specific transmembrane proteins (TPs) (Tepass, 1997). The only known apically localized TP required for the maintenance of cell polarity is the CRB protein of *Drosophila* (Wodarz et al., 1993, 1995; Tepass, 1996). Overexpression and loss-of-function studies show that much of the function of CRB seems to be confined to its short 37 amino acid cytoplasmic domain (Wodarz et al., 1993, 1995). The laterally localized TPs required for the maintenance of epithelial polarity are Cadherins, enriched at AJs (Tepass et al., 1996; Uemura et al., 1996; Yap et al., 1997), and NRX IV, localized to SJs (Baumgartner et al., 1996; M. A. B. and H. J. B., unpublished data). Finally, basally located TPs like integrins play a major role in the interaction with basal substratum and are required for adhesion of epithelial cells to their extracellular environment (Brown, 1993; Hynes, 1996). The activity of each of these proteins causes only a partial polarization, and similarly, loss of any of these proteins leads only to a partial loss of polarity (Tepass, 1997).

In vertebrates, several nontransmembrane proteins have been shown to be associated with AJs and TJs. For example, TJs contain cytoplasmic membrane–associated guanylate kinase family proteins (MAGUKs) (Woods and Bryant, 1993; Anderson, 1996), which typically contain SH3, a guanylate kinase, and PDZ domains (*P*SD-95, *D*iscs Large, and *Z*O-1). The first isolated MAGUK was *Drosophila* Discs Large (DLG) (Woods and Bryant, 1991; Woods et al., 1996). Many proteins containing one or more PDZ domains have been implicated in localizing membrane proteins to specific subcellular regions by interacting with C-terminal amino acid residues of transmembrane proteins (Songyang et al., 1997). However, the mechanisms for protein localization remain largely unknown.

Although many PDZ domain proteins localize to specialized sites (Ponting et al., 1997), only DLG has been shown to be required for the localization of junctional complexes or for the maintenance of apico–basal polarity in epithelial cells. Here, we describe the identification of a novel gene, *discs lost (dlt)*, which encodes a protein with four PDZ domains (DLT). DLT displays a dynamic apico–basal distribution during cellularization and epithelial cell formation, which is thought to be a requirement for an organizer of epithelial polarity. DLT interacts with the C-terminal domain of NRX IV and CRB, and loss of DLT causes a mislocalization of the junction proteins and a concomitant loss of epithelial polarity. Double-stranded RNA (dsRNA) interference of *dlt* resulted in loss of epithelial polarity at cellular blastoderm. Hence, DLT forms protein scaffolds that are required to establish and maintain epithelial polarity.

‖To whom correspondence should be addressed (e-mail: hbellen@bcm.tmc.edu).

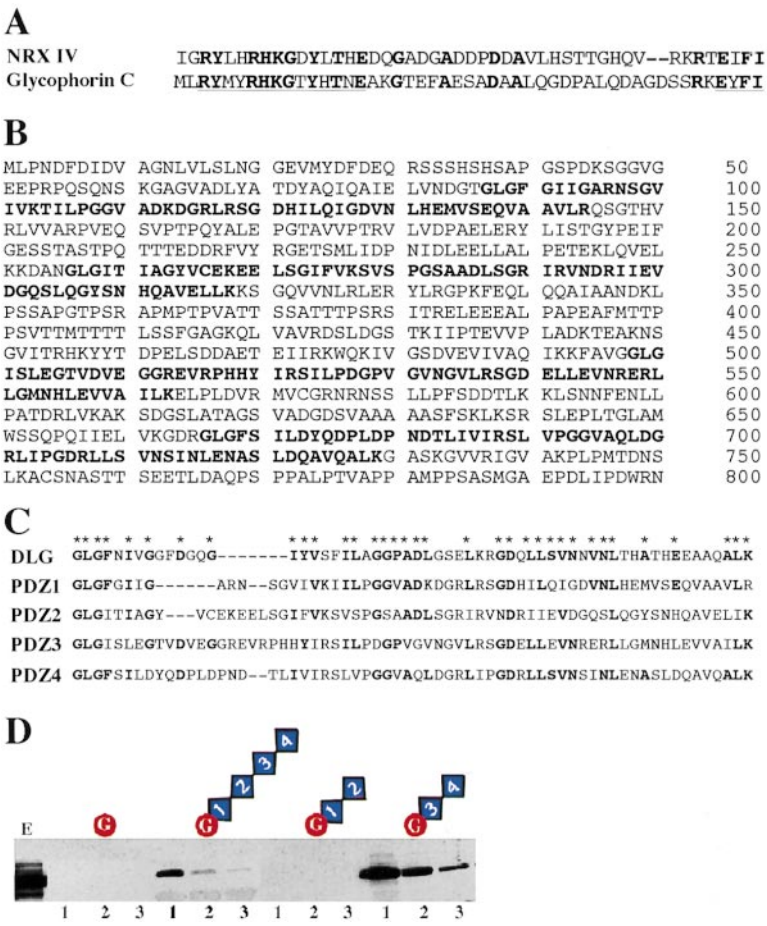

Figure 1. NRX IV Interacts with a Four PDZ Domain–Containing Protein

(A) Sequence alignment between the cytoplasmic 48 amino acids of NRX IV and glycophorin C. Identical amino acids are shown in bold. A Band 4.1 binding consensus sequence at the N terminus (Littleton et al., 1997) and the putative PDZ-binding motif at the C terminus are underlined.

(B) Deduced amino acid sequence of DLT with PDZ domains in bold.

(C) Alignment of domain 1 of DLG and PDZ domains of DLT. Identical amino acids are in bold, and conserved amino acids have an asterisk.

(D) GST and GST fusion proteins containing DLT (G1–4), domains 1 and 2 (G1–2), and domains 3 and 4 (G3–4) were incubated with embryonic extract (E) for 4 hr, and bound proteins were resolved by SDS–PAGE. Immunoblotting with anti-NRX IV showed that NRX IV interacts with full-length DLT protein and domains 3 and/or 4, but does not interact with domains 1 and 2.

Results

NRX IV Interacts with a Protein Containing Four PDZ Domains

NRX IV is a transmembrane protein specifically localized to pleated SJs (pSJs) and required for the formation of intercellular septae characteristic of pleated SJs (Baumgartner et al., 1996; M. A. B. and H. J. B., unpublished data). The cytoplasmic domain of NRX IV shows 68% similarity to the red blood cell transmembrane protein glycophorin C (Figure 1A) that binds to p55 (a MAGUK) with its carboxy-terminal four amino acids (Marfatia et al., 1997; Songyang et al., 1997). These observations suggested that the carboxy-terminal amino acids of NRX IV may bind a protein with PDZ domains.

To identify proteins that interact with the cytoplasmic domain of NRX IV, we carried out a yeast two-hybrid interaction screen using the cytoplasmic 48 amino acids of NRX IV as bait (Durfee et al., 1993). We screened approximately 2×10^6 colonies and isolated 15 positive clones. Seven independent clones showed identical overlapping sequences. Developmental Northern blot analysis using a near full-length cDNA corresponding to the isolated clones showed the presence of a single transcript of about 3.5 kb at all developmental stages. In situ hybridization to embryos showed that the gene is expressed in many epithelial tissues of ectodermal origin, similar to *nrx IV* (data not shown).

As shown in Figures 1B and 1C, the corresponding cDNA (3.2 kb; GenBank #AF103942) encodes a novel protein that contains four PDZ domains, named Discs Lost (DLT, see below). The sequence homology between the first PDZ domain of DLG and those of DLT is shown in Figure 1C. To obtain further evidence for the interaction between NRX IV and DLT, we performed biochemical assays. GST-fusion proteins containing full-length DLT, domains 1 and 2, or domains 3 and 4 were bound to glutathione-matrix and incubated with embryonic extract. NRX IV is retained on the matrix containing full-length protein after extensive washing (Figure 1D), indicating a strong interaction between these proteins. In addition, NRX IV binds to PDZ domains 3 and/or 4, but not to GST and PDZ domains 1 and 2. Hence, the interaction between the cytoplasmic domain of NRX IV and the last two PDZ domains of DLT is specific. The domain of NRX IV that interacts with the third or fourth PDZ domain probably corresponds to the carboxy-terminal amino acids RTEIFI, similar to the motif RKEYFI of glycophorin C (see Figure 1A; Songyang et al., 1997). These data suggest that NRX IV and DLT interact in vitro and possibly in vivo.

DLT Localization Is Dynamic during Early Development

To determine whether the observed interactions between NRX IV and DLT are physiologically relevant, we

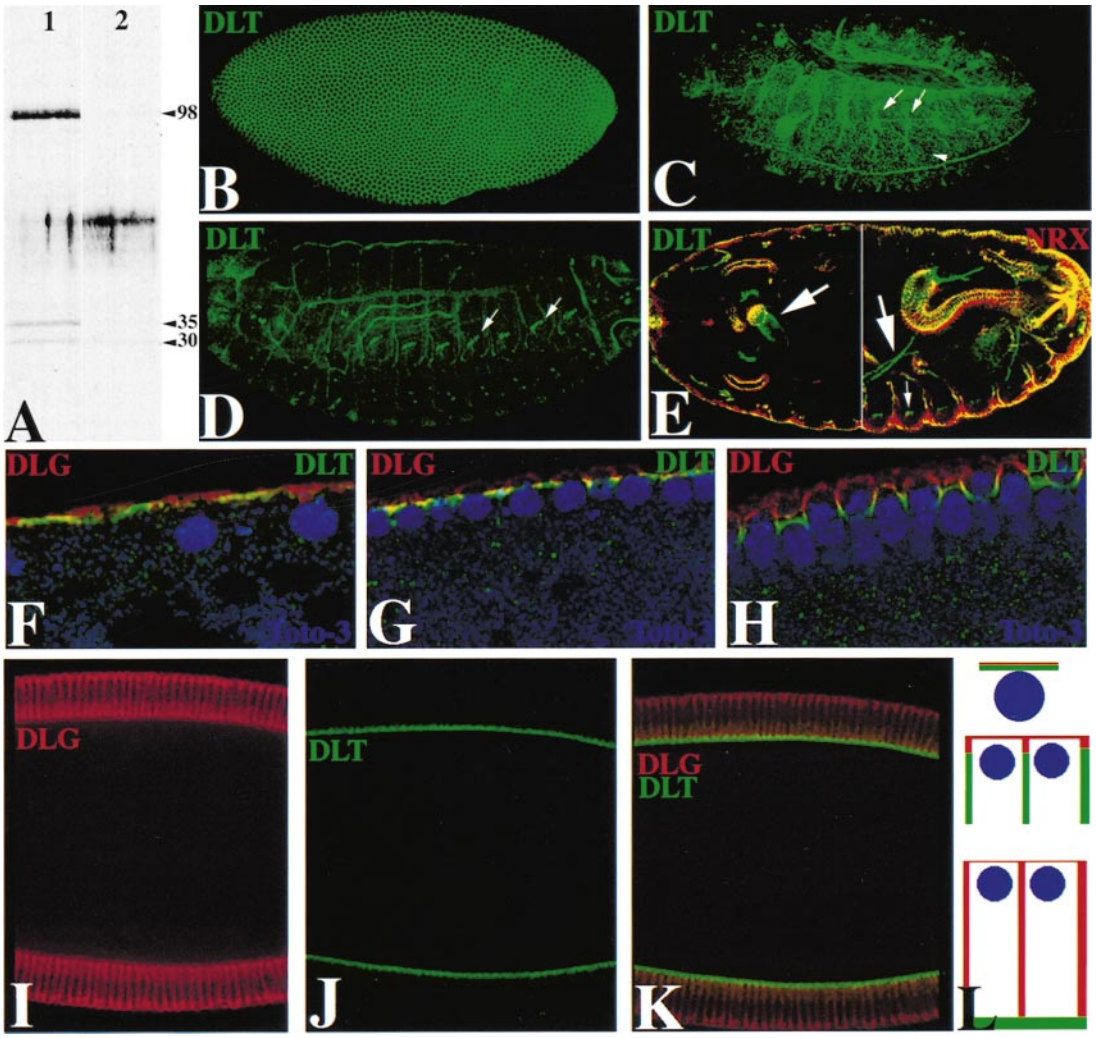

Figure 2. Expression and Localization of DLT

(A) Western blot of single embryos (22- to 23-hr-old) of *Df(3L)APRT126/TM6*, *Tb P{w*$^{+}$*,abdAlacZ}* (lane 1), and *Df(3L)APRT126/Df(3L)APRT126* (lane 2) immunoblotted with rabbit anti-DLT recognizes a predominant protein band migrating at 98 kDa and two small bands at 35 and 30 kDa (lane 1). The 98 kDa band is undetectable and the other bands barely detectable in the homozygous deficiency embryos (lane 2).

(B–D) Immunolocalization of DLT shows that it is expressed prior to cellularization and is membrane associated (B). DLT is more strongly expressed in ectoderm and invaginating tracheal pits than in other cells (arrowhead, arrows [C]). At stage 16, DLT is expressed in trachea and cells of the peripheral nervous system (arrows [D]).

(E) A stage 16 embryo stained with anti-DLT (green) and anti-NRX IV (red). Anterior half, focus is on ectoderm, salivary glands, and posterior end of proventriculus (green, arrow). Posterior half, focus is on ectoderm, hindgut, nervous system (small arrow), and Malpighian tubules (green, arrow). The two proteins are coexpressed in all tissues (yellow and orange) except epithelia that do not contain pleated SJs (e.g., Malpighian tubules and proventriculus).

(F–H) Triple-labeled embryos with anti-DLT (red), anti-DLG (green), and a nuclear stain, Toto-3 iodide (blue). (F) Both DLT and DLG are expressed apically at stage 3. (G) A stage 4 embryo shows that DLT has started to move basally, whereas DLG stays apical. (H) A late stage 4 embryo. DLT protein has moved basally and is at the leading edge of invaginating membranes during cellularization.

(I–K) Wild-type embryo at cellular blastoderm stained with anti-DLG (red) and anti-DLT (green). Note that most DLT immunoreactivity is present on the basal side of the columnar blastoderm cells, whereas DLG is mostly localized laterally.

(L) Summary of expression of DLT during cellularization. Top, cycle 12 or 13; bottom, cycle 14. Color code is the same as in photographs.

first analyzed the expression pattern and subcellular localization of DLT using anti-DLT antibodies. Western blot analysis of wild-type embryos (Figure 2A, lane 1) showed a predominant band of an estimated molecular weight of 98 kDa and two faint bands of 35 and 30 kDa. The smear around 40–45 kDa corresponds to abundant yolk proteins. The size of the 98 kDa protein is in reasonable agreement with the predicted molecular weight of 88 kDa. The two fainter bands are likely to be degradation products of the 98 kDa protein. The 98 kDa band and 35 kDa bands are lacking in the homozygous deficiency embryos (see below), and the 30 kDa band is significantly reduced in these embryos (Figure 2A, lane 2). Since DLT is provided maternally (see below), this faint 30 kDa is probably a degradation product of the maternal component.

Drosophila epithelia have been subdivided into two types: primary and secondary. Primary epithelia are derived from the first epithelium, the cellular blastoderm, without a mesenchymal intermediate, and are characterized by the presence of AJs. They include the ectoderm, foregut, hindgut, tracheal system, subperineurium, peripheral glia, and salivary glands. Secondary epithelia form by a mesenchymal–epithelial transition and lack AJs. They include the midgut and portions of the proventriculus (Tepass and Hartenstein, 1994). As shown in Figure 2B, the DLT protein is present at cellular blastoderm formation. At all subsequent embryonic stages (Figures 2C–2E), DLT is membrane associated and localized to primary and some secondary epithelial cells (e.g, ectodermal cells [arrowhead, Figure 2C], salivary glands, foregut, hindgut, and invaginating tracheal cells [small arrows, Figures 2C and 2E]). In addition, DLT is expressed in specific cells of the peripheral nervous system (arrows in Figure 2D).

Since DLT is expressed during cellularization (Figure 2B), we examined the precise temporal and subcellular localization of DLT in 0- to 3-hr-old embryos (Figures 2F–2H). DLT is first detected faintly in mitotic cycle 11 when the furrows made by the imprint of the embryonic nuclei become apparent. During mitotic cycles 12 and 13, DLT is mostly colocalized with DLG. However, during late cycle 13 and early cycle 14, the localization of DLT and DLG starts to differ, and DLT becomes localized at the leading edge of the invaginating membranes during cellularization (Figure 2H), whereas DLG shows a complementary nonoverlapping localization. After completion of cellularization (Figures 2I–2K), DLT is exclusively localized to the basal area of the columnar epithelial cells. Thus, early expression of DLT indicates that it may be required during cellularization to establish epithelial polarity. A summary of its localization during cycles 12–14 is shown in Figure 2L.

DLT Colocalizes with CRB and NRX IV

The CRB protein is first detected at low levels during early gastrulation in a tight apical and lateral domain (Figure 3A). DLT expression partially shifts from basal to apical during this stage (Figures 3B–3C). When the first traces of CRB protein are observed apically and laterally, some DLT protein colocalizes with CRB in the apico–lateral area, whereas most of the DLT protein is still basal at this stage. At subsequent developmental stages, both proteins colocalize apically, but DLT extends slightly more basal than CRB (Figures 3D–3F). The major difference is that, unlike CRB, DLT is provided maternally and present prior to and during cellularization. At later stages, CRB and DLT overlap extensively in embryonic and larval tissues (see below). To determine whether loss of *crb* had any effect on the localization of DLT, *crb* mutant embryos were double labeled with anti-CRB and anti-DLT. As shown in Figures 3G–3I, DLT fails to localize to the apical side in the absence of CRB protein and is distributed over the entire cell membrane and cytoplasm in embryos that lack CRB. Hence, DLT depends on CRB for its proper subcellular localization at later developmental stages.

As shown in Figure 2E, most epithelial cells coexpress NRX IV and DLT. To precisely determine where DLT is localized with respect to NRX IV, we double labeled stage 13–16 embryos with antibodies against DLT, NRX IV, and DE-Cadherin (DE-CAD) (Oda et al., 1994; Uemura et al., 1996). NRX IV and DLT only overlap at the most apical portion of the SJs (Figures 3J and 3K). At this resolution, it is not possible to determine whether the proteins abut or overlap at the SJs. However, DLT clearly extends apically of the SJs, where it colocalizes with DE-CAD (Figure 3L). We conclude that DLT is a membrane-associated protein covering the apical site of pleated SJs, the AJs, and the apical domain as summarized in Figure 3M. Our data also suggest that DLT and NRX IV interact in vivo and that this interaction is confined to the most apical domain of the SJs.

DLT and CRB Interact Directly

The apical localization of DLT and CRB suggests that DLT may interact with CRB. As previous studies showed that deletion of 23 carboxy-terminal amino acids of the CRB protein leads to a null mutant phenotype (Wodarz et al., 1993, 1995), we investigated whether the two proteins interact using a GST-CRB fusion protein containing the 37 cytoplasmic amino acids of CRB. GST pull down experiments showed that full-length T7-tagged DLT interacts with the cytoplasmic domain of CRB (GST-CRB) (Figure 3N). However, DLT that lacks the first PDZ domain fails to bind GST-CRB (data not shown), suggesting that the first PDZ domain is required for CRB binding. In addition, DLT from adult extracts also bound to GST-CRB (data not shown), indicating that both proteins bind to each other in vivo.

The subcellular localization of DLT suggests that it forms a protein scaffold by homotypic interaction as previously shown for other PDZ domain–containing proteins. We therefore determined whether DLT protein can bind to the PDZ domains 1–4, 1–2, or 3–4 of DLT immobilized to GST beads. As shown in Figure 3N, the T7-tagged DLT binds to the full-length protein (domains 1–4) and domains 3–4 but fails to bind to domains 1–2. These data suggest that DLT can form homomultimers through its PDZ domains 3 and/or 4.

Mutational Analysis of *dlt* Reveals a Complex Locus

To determine the in vivo function of *dlt*, we initiated a genetic analysis. *dlt* was mapped to 62B3–6, a region that was previously saturated with chemically and γ-ray-induced mutations (Sliter et al., 1989; Wang et al., 1994). Using Southern analysis and in situ hybridization experiments, *dlt* was mapped between the break points of *Df(3L)APRT126* (62B2–4;B10–11) and *Df(3L)R^{E}* (62B7-B12) (Figure 4A). This region contains three essential complementation groups: *dre1*, *dre3*, and *cdc37* (Sliter et al., 1989; Cutforth and Rubin, 1994). *dre3* corresponds to the α-*spectrin* gene (Lee et al., 1993; Wang et al., 1994), and *cdc37* is located next to α-*spectrin* (Cutforth and Rubin, 1994), suggesting that the gene encoding DLT is *dre1*.

To establish that the *dre1* complementation group corresponds to *dlt*, we isolated cosmids using the *dlt* cDNA as a probe (Tamkun et al., 1992). Two cosmids (COSMY8-1 and COSMY1-1) fully rescued the lethality of *dre1*. Both cosmids overlap by approximately 10 kb

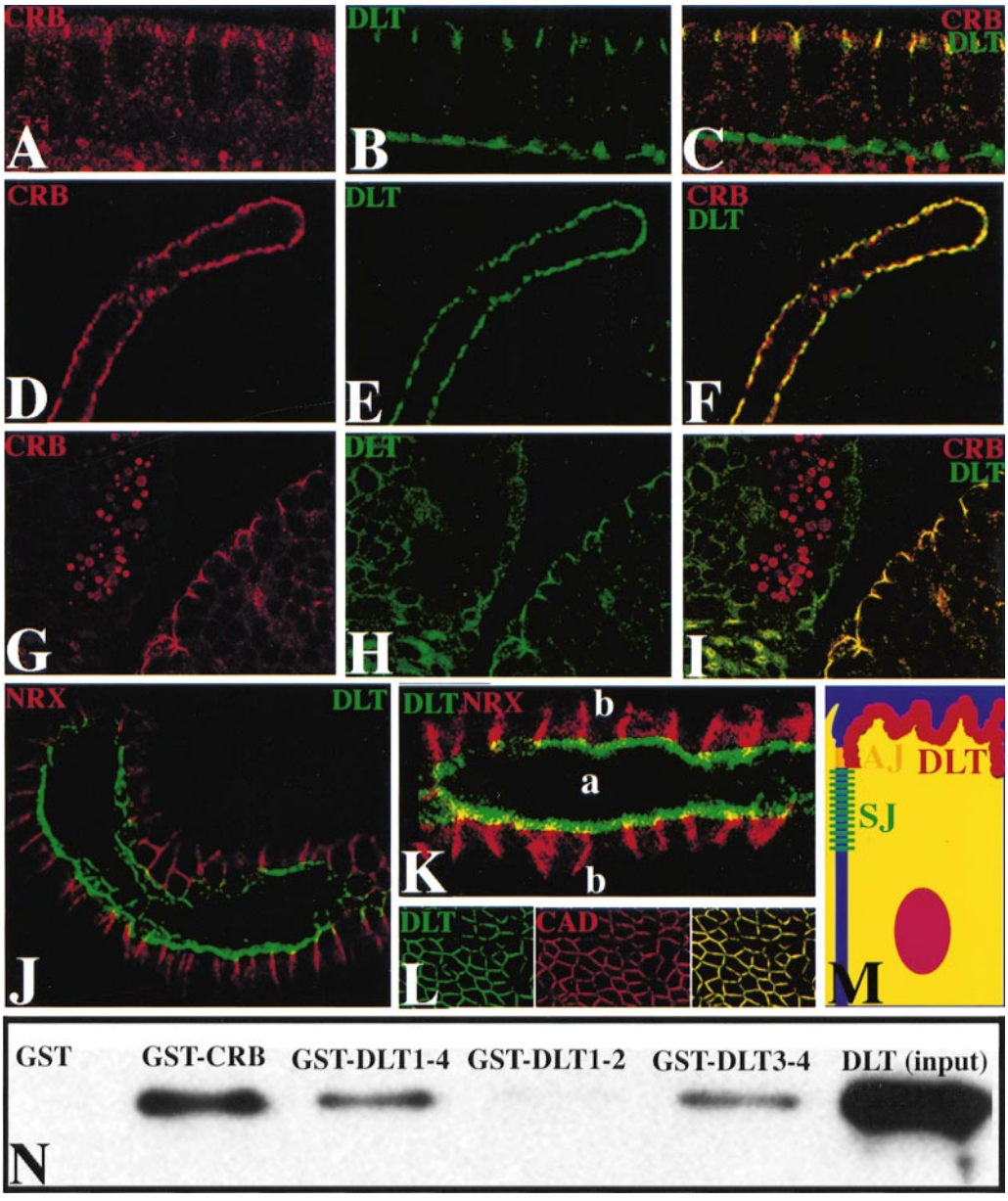

Figure 3. DLT Shows a Dynamic Apico–Basal Expression and Interacts with CRB

(A–C) A wild-type gastrulating embryo (~3 hr, 10 min) double stained with anti-CRB (red) and anti-DLT (green). This is the earliest time point at which we detect CRB expression, and it coincides with the apical movement of DLT. Both proteins colocalize at the apico–lateral area. Most of the DLT is still localized basally.

(D–F) A portion of the salivary gland from a stage 16 embryo shows that DLT and CRB mostly colocalize in the apical region.

(G–I) Wild-type (right) and *crb* mutant (left) stage 7 embryos stained with anti-CRB ([G], red) and anti-DLT ([H], green) and overlay (I). Wild-type embryo ([G], right) shows localization of CRB to the apical area of epidermal cells. *crb* mutants ([G], left) lack CRB immunoreactivity. In *crb* mutant embryos, DLT fails to localize to the apical area of epidermal cells ([H], left) but is diffusely localized to the cortical area of the cells.

(J) A portion of the hindgut from a stage 16 embryo double stained with anti-DLT (green) showing apical localization of the protein that corresponds to the lumen of the hindgut, and anti-NRX IV (red) localized to SJs at a higher magnification. DLT and NRX IV are expressed in the same cell and are in close proximity to each other. In many cells there is a yellow dot in the apical domain of NRX IV expression, indicating a domain of overlap.

(K) A portion of a salivary gland of a stage 16 embryo double stained with anti-DLT (red) and anti-NRX IV (green). a, apical; b, basal.

(L) Coimmunolocalization of DLT (green) with the adherens junction–specific protein DE-CAD (red). Both proteins are mostly colocalized.

(M) Schematic representation of the subcellular localization of DLT with respect to AJs and SJs. DLT forms a cap at the apical area of the epithelial cell.

(N) GST pull down assay using GST (lane 1) and a fusion protein of GST with the intracellular domain of CRB. T7-tagged DLT was able to bind to the fusion protein in vitro (lane 2). DLT also bound to GST with full-length DLT (lane 3) and GST with domains 3 and 4 (lane 5) but showed no binding with a fusion protein containing GST with domains 1 and 2 (lane 4). The amount of T7-tagged DLT used in these assays (input) is shown in lane 6.

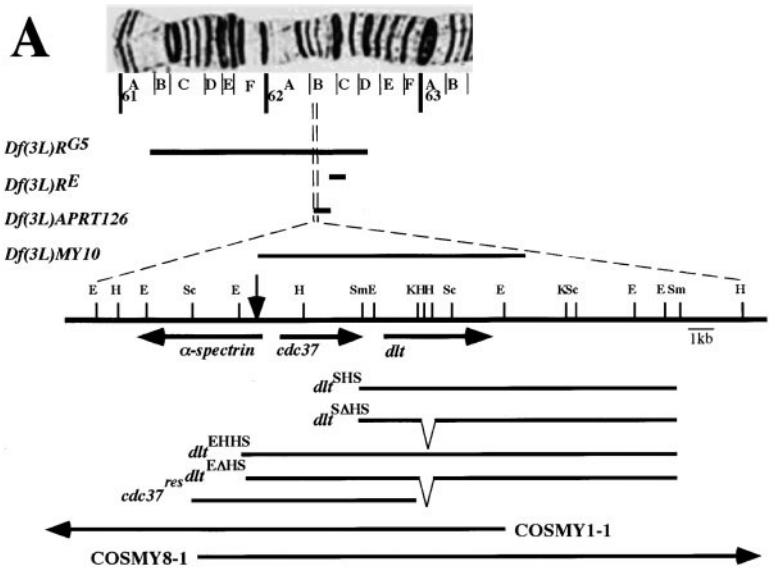

B

Deficiency / Transgenic Line	*dre1*	*cdc37*	α-*spectrin*
Df(3L) APRT126	-	-	-
Df(3L)MY10	-	-	+
P{w+-cosMY1-1}	+	+	+
P{w+-cosMY8-1}	+	+	-
P{w+-cdc37res}	-	+	-
P{w+-dltEHHS}	+	+	-
P{w+-dltEΔHS}	-	+	-
P{w+-dltSHS}	+/-	-	-
P{w+-dltSΔS}	-	-	-

Figure 4. Genetics of *discs lost*

(A) Portion of polytene chromosome and deficiencies that uncover the 62B region containing the *discs lost* gene. A 22 kb genomic region contains three genes: *cdc37* (Cutforth and Rubin, 1994), a portion of α-*spectrin* (Lee et al., 1993; Wang et al., 1994), and *dlt*. Transcripts are indicated by horizontal lines with arrows showing the direction of transcription. Vertical arrow on the genomic walk indicates the position of $P^{595/4}$ insertion. Its mobilization resulted in the deletion of about 10 kb to the right of the insertion, generating the deficiency *Df(3L)MY10* that uncovers *cdc37* and *discs lost*. The breaks in the horizontal lines indicate an internal deletion in the rescue constructs utilizing the two HindIII sites within the coding sequence of the *dlt* gene.

(B) Summary of the complementation data and ability of various genomic rescue constructs to complement mutations in *dlt* (=*dre1*), *cdc37*, and α-*spectrin*. +, complements or completely rescues; −, does not complement or does not rescue; +/−, fully formed pharate adults.

and contain a portion of the α-*spectrin* gene, the entire *cdc37* gene, and the genomic region encoding DLT. COSMY8-1 only rescued mutations in *cdc37* and *dre1*, further suggesting that *dre1* corresponds to *dlt*. To demonstrate that *dre1* affects *dlt* only, we attempted to rescue the phenotypes associated with *dre1* (see below) with a 10 kb SmaI/SmaI (SHS) and a 15 kb EcoRI/SmaI (EHHS) genomic fragment (Figure 4). The 10 kb fragment provided a weak partial rescue, whereas the 15 kb (includes *cdc37*) caused a strong partial rescue (Figure 4). To rule out the possibility that another gene was affected in the *dre1* mutant chromosome, we generated small internal deletions of the ORF of *dlt* (SΔHS and EΔHS) that failed to rescue *dre1*. These data demonstrate that *dre1* mutation affects *dlt*.

To isolate other alleles of *dlt*, we identified a P element, $P\{w^+,lacZ\}^{595/4}$ (62B2–4; Salzberg et al., 1997), which failed to complement *dre1* but complemented α-*spectrin* and *cdc37* null mutations. The lethality associated with $P\{w^+,lacZ\}^{595/4}$ can be reverted to wild type by excision (data not shown), demonstrating that it is responsible for the mutation. Hence, $P\{w^+,lacZ\}^{595/4}$ is an allele of *dre1* inserted in an intron of the α-*spectrin* gene (arrow in Figure 4). These data are in agreement with the rescue data, since the 10 kb SmaI/SmaI (SHS) fragment rescues poorly, the 15 kb EcoRI/SmaI (EHHS) fragment almost fully rescues, whereas COSMY1-1 provides a full rescue (Figure 4). Hence, a regulatory element of *dlt* resides approximately 5 kb upstream of its putative initiation site, within an intron of α-*spectrin*. In addition, our data indicate that this regulatory element is not required for *cdc37* and α-*spectrin*.

To generate null mutations of *dre1*, we generated imprecise excisions of $P\{w^+,lacZ\}^{595/4}$, creating a 10 kb deficiency, *Df(3L)MY10* (Figure 4). This deficiency complements mutations in α-*spectrin* but fails to complement mutations in *dre1/dlt* and *cdc37*. To determine the null phenotype associated with the loss of *dlt*, we rescued the lethality of the *cdc37* gene with a genomic fragment harboring *cdc37*, previously shown to rescue null alleles of *cdc37* (Cutforth and Rubin, 1994). $P\{w^+,cdc37^{res}\}/P\{w^+,cdc37^{res}\}$; *Df(3L)MY10/Df(3L)MY10* animals die as first/second instar larvae. Larval lethality can be rescued to a late pupal lethality with fully developed pharate adults with the 15 kb EcoRI/SmaI (EHHS) construct, showing that the lethality is due to the loss of *dlt*. In summary, we have isolated three different *dlt* mutations: two hypomorphic alleles, *dre1* and $P\{w^+,lacZ\}^{595/4}$, and a null allele, *MY10*. In addition, we have demonstrated that this gene is associated with key regulatory sequences nested in an intron of the α-*spectrin* gene that is separated from the gene encoding DLT by *cdc37*.

Mutations in *dlt* Affect Imaginal Discs

As shown in Table 1, null mutations $P\{w^+;cdc37^{res}\}/\{w^+;cdc37^{res}\}$; *Df(3L)MY10/Df(3L)MY10* or $P\{w^+;cdc37^{res}\}/\{w^+;cdc37^{res}\}$; *Df(3L)MY10/D(3L)APRT126* cause mostly

Table 1. Phenotypes of Various *dlt* Alleles and Allelic Combinations

Allele/Genotype	Lethal Stage/Phenotype
dlt^{dre1}/dlt^{dre1}	Pupal lethal
dlt^{dre1}/*Df(3L)APRT126*	Third instar/early pupal lethal, no discs
dlt^{dre1}/*Df(3L)MY10*	Third instar/early pupal lethal, no discs
$dlt^{595/4}/dlt^{dre1}$	Fully developed pupae with leg duplications
$dlt^{595/4}$/*Df(3L)APRT126*	Second instar
$dlt^{595/4}/dlt^{595/4}$	First/second instar
dlt^{MY10},$P\{w^+, cdc37^{res}\}$/*Df(3L)APRT126*	First/second instar

first instar lethality, with few second instar escapers. Homozygous $P\{w^+, lacZ\}^{595/4}$ and $P\{w^+, lacZ\}^{595/4}$/*Df(3L)MY10* are second instar lethals. Homozygous *dre1* animals die after pupation and completely histolyse, whereas *dre1*/*Df(3L)MY10* animals die mostly as late third instar larvae. Finally, *dre1*/$P\{w^+, lacZ\}^{595/4}$ animals die as late pupae, undergo metamorphosis, but fail to eclose, suggesting some interallelic complementation. Many larvae lack imaginal discs, with the exception of the eye-antennal disc (data not shown). Based on this phenotype, we named the gene *discs lost* (*dlt*), in contrast to *discs large* (Woods and Bryant, 1991). The lack of an overt phenotype in null mutant embryos is due to the presence of maternal DLT (see below).

dlt dsRNA–Mediated Interference of *dlt* Expression Causes Loss of Epithelial Polarity

DLT is expressed abundantly in ovaries (data not shown). To assess the consequences of the loss of maternal DLT in embryos, we used the dominant female sterile technique (Chou and Perrimon, 1992). However, we were unable to recover females that laid any eggs, even though more than 50% of the control females produced eggs. Hence, DLT is essential for oogenesis. To circumvent the inability to produce eggs with reduced maternal DLT, we resorted to dsRNA interference, previously shown to be effective in *C. elegans* and *Drosophila* (Fire et al., 1998; Kennerdell and Carthew, 1998). dsRNAs were directed against the 5′- and 3′-untranslated (UTR) sequences or against sequences in the ORF of *dlt*. dsRNA for *lacZ* coding sequences and injection buffer served as controls. Embryos treated with dsRNA for *lacZ* and/or injection buffer did not reveal any developmental defects (Figure 5A). *dlt* dsRNA–injected embryos express very low levels or no DLT (Figure 5B). More importantly, 3- to 4-hr-old injected embryos lack the columnar cell morphology. Instead, the epithelium consists of small cuboidal cells that are about one-fourth the length of those of control embryos. These cells have completed cellularization, as low levels of DLT and DLG are present in the basal area (data not shown). However, unlike control embryos where DLG is localized laterally, DLG is localized apically and laterally. These observations, combined with the expression pattern of DLT, indicate that DLT is required to establish epithelial polarity during cellular blastoderm formation.

Since CRB is expressed after cellular blastoderm, at the onset of gastrulation, injected embryos were aged to germband extension (stage 11) and immunostained with anti-DLT and anti-CRB. *lacZ* dsRNA–injected embryos developed normally and showed no defects in cellularization and localization of DLT or CRB (Figures 5C–5E). However, *dlt* dsRNA–injected embryos fail to express DLT (Figure 5F) but express CRB (Figures 5G and 5H). At higher magnification, control-injected embryos show normal cell morphology and localization of cell junction–specific proteins (Figure 5I), but *dlt* dsRNA–injected embryos display a completely aberrant CRB localization and embryo morphology. Thus, removal of DLT prior to cellularization causes a complete lack of polarity based on morphological features and CRB localization.

DLT Is Required to Maintain Epithelial Cell Polarity

Immunohistochemical staining and Western blot analysis (Figure 2A) showed that *dlt* null mutant embryos exhaust maternal DLT during stage 16. To determine whether lack of DLT affects localization of NRX IV in these embryos, we stained them with anti-DLT and anti-NRX IV antibodies. As shown in Figure 6A, salivary glands of stage 16 null mutants lack DLT, and NRX IV becomes gradually localized to the apical domain (Figure 6B). This aberrant apical localization of NRX IV was never observed in wild-type cells (see Figures 2F and 2G). Similar defects were also observed in other tissues (data not shown). Therefore, DLT is required to maintain the demarcation of the apical boundary of SJs and restricts the localization of NRX IV to the lateral domain. These observations indicate the first features of the demise of the apical surface and the breakdown of the AJs.

Next we analyzed partial loss-of-function *dlt* mutants in the giant cells of the third instar salivary gland. These cells have prominent SJs and AJs, and the apical domain is easily identified as the luminal area. As shown in Figures 6C–6E, wild-type salivary glands contain SJs (Figure 6C; see also Woods et al., 1996), and CRB is restricted to the apical/luminal domain (Figure 6D; Tepass et al., 1990; Wodarz et al., 1995). Double labeling using anti-NRX IV and anti-CRB showed that both proteins are mislocalized in *dlt* mutant salivary gland cells (Figures 6F–6H). The cells do not maintain their epithelial organization, and NRX IV localization is aberrant; instead of being baso–lateral, the protein is localized to the entire cell membrane and enriched at the former luminal (apical) domain. In addition, CRB localization is diffuse (Figure 6G). Some of the CRB protein is still membrane associated, but a significant portion is cytoplasmic, similar to *crb* mutants that lack the carboxy-terminal domain (Wodarz et al., 1993).

Most homozygous dlt^{dre1} and transheterozygous dlt^{dre1}/*Df(3L)APRT126* wandering third instar larvae exhibit obvious morphological changes in salivary gland cells. Instead of the typical hexagonal appearance of wild-type cells (Figure 6J), mutant cells are round and lack their normal epithelial morphology and structure. These cells also show a diffuse localization of DLT and Armadillo (compare Figures 6I and 6J). This phenotype is not ob-

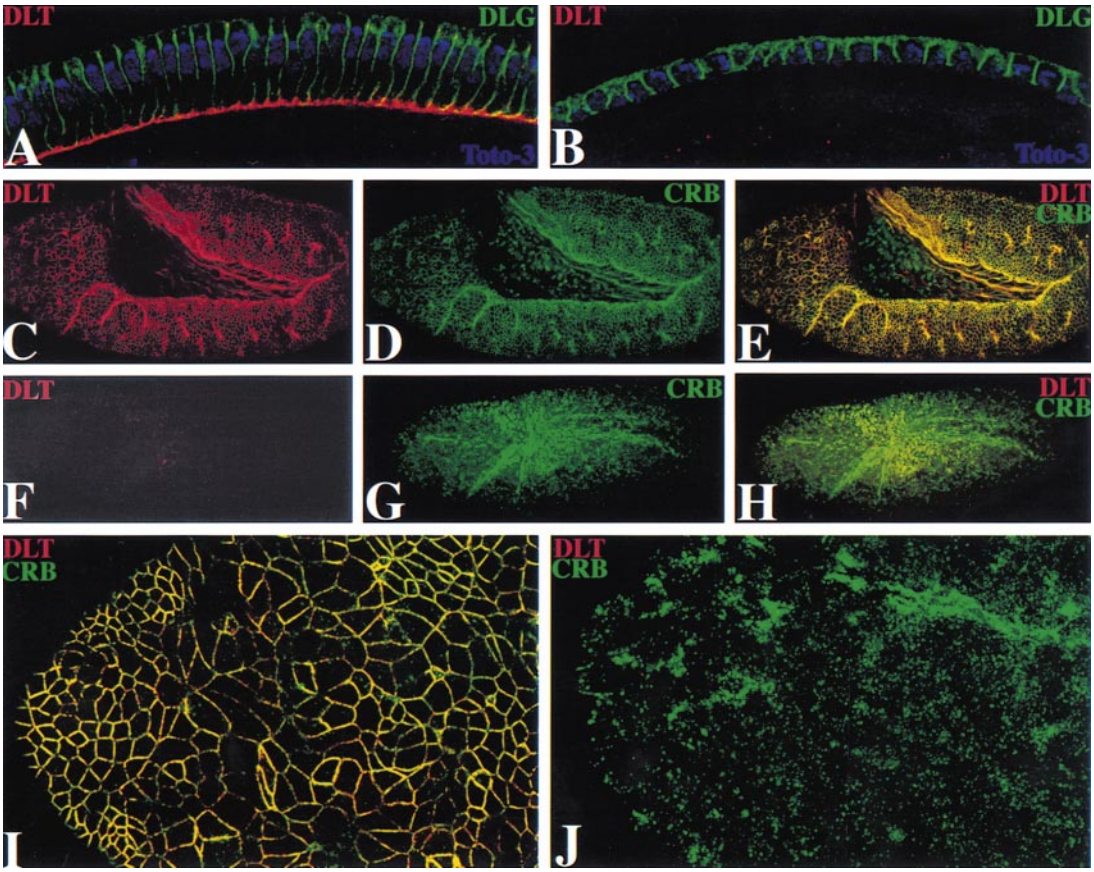

Figure 5. *dlt* dsRNA Abolishes *dlt* Expression and Disrupts Epithelial Polarization

(A) Wild-type cellular blastoderm embryo injected with *lacZ* dsRNA at 0–40 min after egg lay and allowed to develop at 25°C for 3 hr, fixed and triple stained with anti-DLT (red), anti-DLG (green), and a nuclear stain (blue). *lacZ* dsRNA has no effect on localization of DLT to the basal side and DLG to the apical and lateral sides of the columnar blastoderm cells.

(B) A wild-type embryo injected with *dlt* dsRNA at 0–40 min and allowed to develop at 25°C for 3 hr, fixed and stained. DLT immunoreactivity is undetectable, and DLG localizes to the apical and lateral surfaces, but the cells never form a columnar epithelium.

(C–E) Wild-type embryo injected with *lacZ* dsRNA and allowed to develop for 6 hr, fixed and immunostained with anti-DLT ([C], red), anti-CRB ([D], green), and overlay (E).

(F–H) A wild-type embryo injected with *dlt* dsRNA and allowed to develop for an additional 6 hr, fixed and stained with anti-DLT ([F], red), anti-CRB ([G], green), and overlay (H). DLT immunoreactivity is abolished, and CRB is not localized properly.

(I and J) Higher magnifications of (E) and (H), respectively. Both DLT and CRB colocalize and decorate the cell boundaries (I), but no cell boundaries are visible and CRB localization is disrupted (J). The dsRNA-injected embryos shown here represent at least 50%–60% of the embryos injected. The phenotypes observed vary according to the levels of DLT loss.

served in young third instar larvae. The gradual loss of polarity is similar to that observed in *crb* mutant embryos (Tepass et al., 1990; Wodarz et al., 1995), further indicating that *dlt* mutant cells have lost their apico–basal polarity. These observations show that DLT is required for the maintenance of NRX IV and CRB localization and, hence, epithelial polarity.

Ectopic Expression of *dlt* Disrupts Cell Polarity and Epithelial Morphology

To determine whether ectopic *dlt* expression affects epithelial polarity, we used the *hs-GAL4/UAS-dlt* bipartite system (Brand and Perrimon, 1993). Four- to seven-hour-old embryos that received a 1 hr heat shock at 37.5°C did not survive, whereas heat-shocked control embryos showed no lethality. The distribution of DLT and CRB in ectodermally derived epithelia of control embryos is not altered by heat shock alone, and both proteins are localized apically (Figure 7A). However, overexpression of *dlt* (Figure 7B) leads to an irregular epithelial cell layer with abnormally shaped cells that cannot maintain an epithelial context. We also observe a redistribution of CRB localization to basal and baso–lateral areas in some cells that overexpress DLT (Figure 7B, arrows). These data indicate that epithelial polarity is at least partially lost in the presence of additional DLT protein, possibly because of the aberrant distribution of CRB.

Overexpression of DLT causes other defects than CRB mislocalization. DE-CAD staining is barely detectable in these embryos, suggesting that epithelial cell junctions are also compromised (Figures 7C–7D). This is further supported by the subcellular localization of NRX IV. Most embryos that overexpress DLT fail to reach

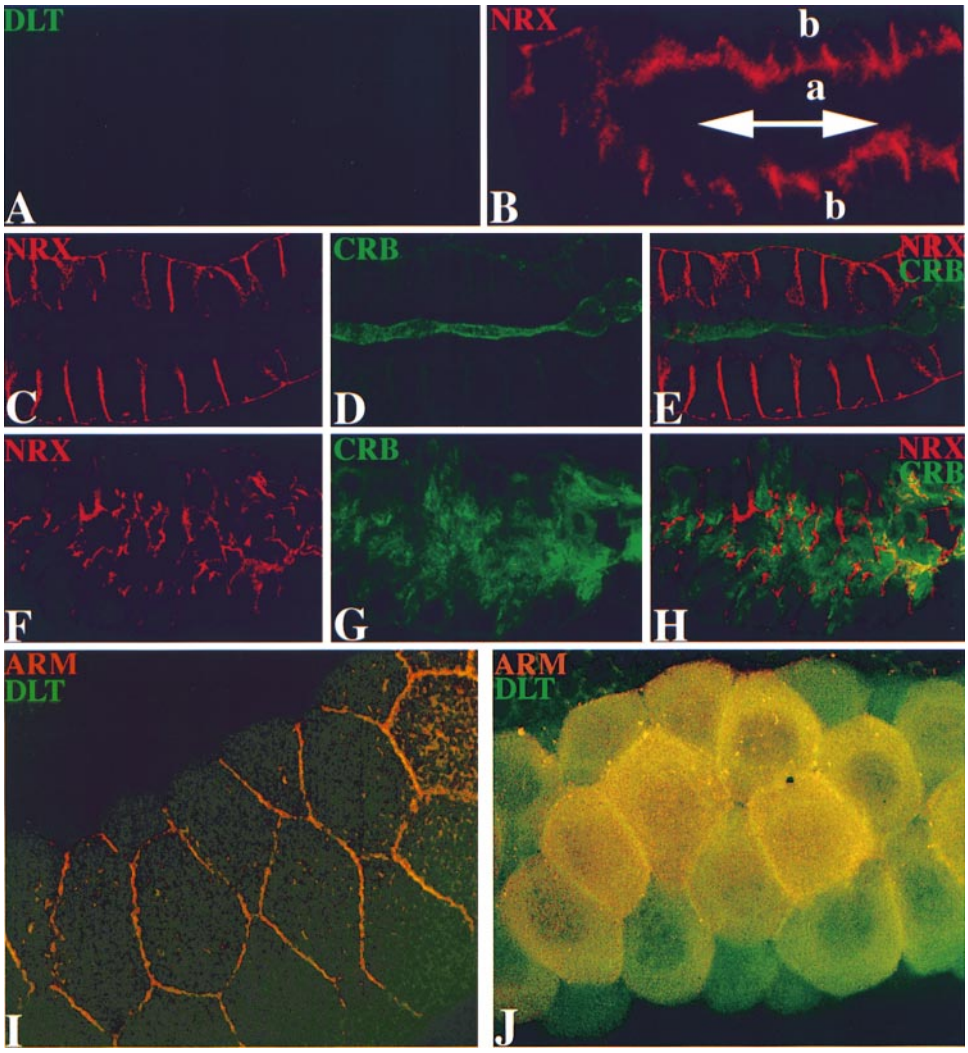

Figure 6. *dlt* Mutants Show Loss of Epithelial Polarity

(A and B) Portion of a salivary gland from a stage 16 null mutant embryo double stained with anti-DLT and anti-NRX IV (compare with Figure 2F). There is no immunoreactivity for DLT, and NRX IV ([B], red) extends more apically, indicating that DLT is required to restrict NRX IV to SJs.

(C–E) Salivary glands from wild-type third instar larvae stained with anti-NRX IV (red) and anti-CRB (green). NRX IV localizes to SJs, whereas CRB is localized to the apical (luminal) region.

(F–H) *dlt* mutant salivary gland displays a loss of cell polarity. The cells have lost the columnar morphology and are almost round. NRX IV is enriched toward the luminal side. CRB, on the other hand, is not restricted to the luminal area but has diffused throughout membrane and cytoplasm (compare [E] and [H]).

(I) A portion of a salivary gland from a wild-type third instar larva stained with anti-DLT (green) and anti-Armadillo (red) showing hexagonal arrays.

(J) A portion of a salivary gland from a dlt^{dre1}/*Df(3L)APRT126* larva stained with anti-DLT (green) and anti-Armadillo (red) showing cells with rounded morphology and diffused staining.

stage 12 when NRX IV expression is first detected. However, some embryos develop beyond stage 12 if they express relatively low levels of additional DLT. NRX IV is then partially redistributed to basal regions of epithelial cells in these embryos (Figures 7E and 7F). This basal subcellular distribution is the opposite of what we observe in loss-of-function embryos, where NRX IV is localized apically (Figure 6), suggesting that DLT reverses polarity when overexpressed. These data suggest that ectopically expressed DLT protein alters the distribution of apical- and cell junction–specific proteins leading to a loss and/or reversal of cell polarity due to reorganization of the protein complexes including CRB, NRX IV, and other DLT-interacting proteins.

Discussion

Role of DLT in Initiation of Epithelial Polarity

The polarity of the blastoderm epithelium is established during cellularization, when a columnar epithelium is formed (Foe et al., 1993; Schejter and Wieschaus, 1993).

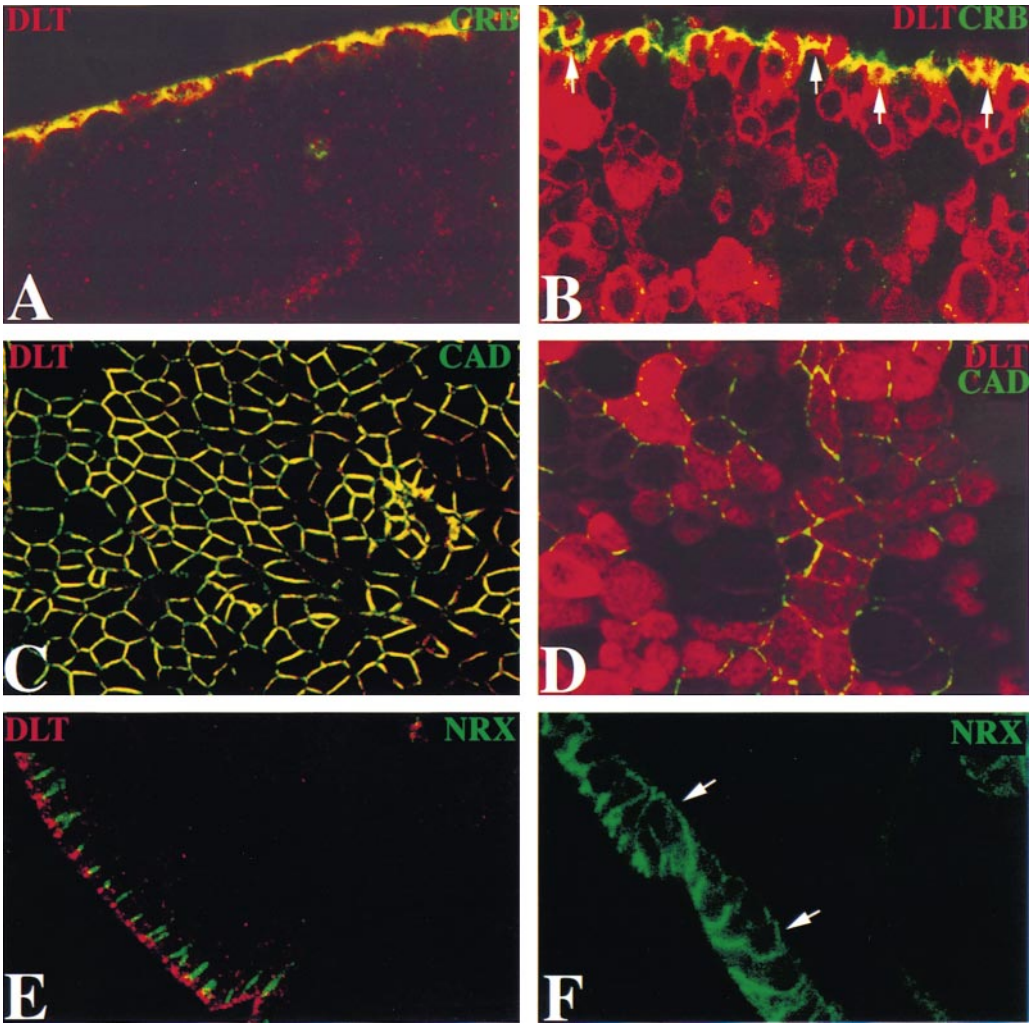

Figure 7. Ectopic Expression of *dlt* Disrupts Epithelial Polarity and Organization

(A) A portion of the ectoderm of a stage 11 control embryo double stained with anti-DLT (red) and anti-CRB (green) showing apical localization of the two proteins.

(B) A portion of ectoderm of a *P{w*$^+$*,hs.GAL4}*,*P{w*$^+$*,UAS-dlt}*/*P{w*$^+$*,hs.GAL4}*,*P{w*$^+$*,UAS-dlt}* embryo stained with anti-DLT (red) and anti-CRB (green) shows a severe disruption of epithelial morphology. The CRB protein does not maintain its apical localization but is redistributed to basal and lateral regions of cells (arrows). Many cells fall out of the epithelial context.

(C) Portion of ectoderm from a stage 11 control embryo and (D) from *P{w*$^+$*,hs.GAL4}*,*P{w*$^+$*,UAS-dlt}*/*P{w*$^+$*,hs.GAL4}*, *P{w*$^+$*,UAS-dlt}* embryo double stained with anti-DLT (red) and anti-DE-CAD (green).

(D) The normal cellular morphology and colocalization of the two proteins at the AJs (C) are disrupted. The DE-CAD levels are severely reduced, and the signal for FITC chromophore was enhanced.

(E) A portion of the ectoderm from a stage 15 control embryo and (F) from *P{w*$^+$*,hs.GAL4}*,*P{w*$^+$*,UAS-dlt}*/*P{w*$^+$*,hs.GAL4}*, *P{w*$^+$*,UAS-dlt}* embryo stained with anti-DLT (red, not shown in [F]) and anti-NRX IV (green). DLT reaches the SJs and colocalizes with NRX IV in a very narrow region.

(F) Epithelial cells show abnormal morphology and apico–basal distribution of NRX IV, which now covers more apical and basal regions of the cells (arrows). The SJ localization of NRX IV is partially maintained.

Beginning of cellularization is marked by invaginations of the egg membrane surrounding each nucleus. As the epithelial sheet is constructed from the apical pole downward, the proteins that initially determine polarity should localize to the egg cortex, the future apical domain of these cells (Tepass, 1997). The process of cellularization is dependent on microtubules and F-actin, and the phenotypes associated with a number of genes required for cellularization have been attributed to cytoskeletal defects (Foe et al., 1993; Schejter and Wieschaus, 1993; Tepass, 1997). Many cells of the blastoderm maintain epithelial polarity during subsequent development, giving rise to primary epithelia. These epithelia gradually acquire AJs, SJs, and a basement membrane (Tepass and Hartenstein, 1994; Cox et al., 1996; Muller and Wieschaus, 1996), thereby establishing a typically polarized epithelium. Previously, the *stardust*, *bazooka*, and *armadillo* genes have been shown to be required for the formation of the zonula adherens (Cox et al., 1996; Muller and Wieschaus, 1996).

The subcellular localization of DLT to the preblastoderm cortical membrane during mitotic cycles 12 and 13, and to the leading edge during membrane invagination at cellular blastoderm formation in cycle 14, suggests that the protein plays a role in organizing apico–basal polarity prior to and during cellular blastoderm formation. The *dlt* dsRNA injection experiments strongly support this hypothesis, as cells with very reduced levels of DLT are short and cuboidal rather than columnar. In addition, mutant epithelial cells maintain a significant apical localization of DLG, not observed in control and wild-type embryos. Furthermore, during early gastrulation, DLT normally colocalizes with CRB. However, embryos that lack DLT fail to polarize as judged by the complete mislocalization of CRB. We conclude that DLT is required to initiate epithelial polarization, and that its absence causes lack of apical and lateral markers to be targeted properly. Hence, DLT seems to establish cell polarity and is the earliest known player in the process of epithelial polarization.

Role of DLT in Maintenance of Epithelial Polarity

Maintenance of polarizing activity requires transmembrane proteins like Cadherins, CRB, NRX IV, and integrins (Tepass, 1997; M. A. B. and H. J. B., unpublished data). CRB is distinct, as it is the only known apically localized protein (Tepass et al., 1990; Wodarz et al., 1995), but *crb* mutant cells do acquire some of the properties of polarized cells (Tepass, 1997). Loss of DLT causes much more severe defects than those observed in *crb* mutants. In addition, DLT is not only required to establish polarity early and to localize CRB properly, but also to maintain CRB localization in the apical domain. At a later stage of development, when NRX IV expression becomes apparent, DLT is also required to maintain its localization. Surprisingly, maintenance of apical DLT localization depends on the presence of CRB, indicating a mutual dependence between DLT and CRB for proper localization at later developmental stages. Finally, overexpression of DLT after cellularization often causes a basal localization of CRB and NRX IV, suggesting that in the presence of extra DLT, epithelial polarity may be at least partially reversed. In addition, dramatic changes in cell morphology, localization of AJ proteins, and loss of epithelial integrity are observed upon overexpression of DLT. Taken together, these data support that DLT is a key determinant of cell polarity.

DLT Interacts with CRB and NRX IV

How does DLT act? We have shown that DLT contains PDZ domains and directly interacts with the carboxy-terminal domain of CRB and NRX IV. Both CRB and NRX IV exhibit structural and functional similarities: large extracellular domains with EGF repeats and Laminin G domains, and short cytoplasmic domains that interact with DLT (Bellen et al., 1998). Interestingly, most of the CRB protein function has been assigned to its cytoplasmic 37 amino acids (Wodarz et al., 1995). In addition, loss of the carboxy-terminal amino acids of CRB or NRX IV leads to a null mutant phenotype (Wodarz et al., 1993; M. A. B. et al., unpublished data). Finally, both NRX IV and CRB are coexpressed in most epithelial cells and play a role in epithelial differentiation (Tepass et al., 1990; M. A. B. and H. J. B., unpublished data). Given the importance of the cytoplasmic domains of NRX IV and CRB, and their ability to bind DLT, we propose that DLT binding is important for the targeting and the maintenance of several protein complexes required for polarized epithelia.

Since CRB and NRX IV are not expressed during cellularization, DLT probably interacts with other proteins to establish polarity during cellularization. During gastrulation, DLT may first form a complex with CRB to target it to the apical domain. This interaction may be essential to maintain apical identity, as loss of either protein causes loss of polarity. In a second phase, DLT is required for the proper localization of the components of the AJs. The protein is prominent in these junctions, but we have not found a molecular partner for DLT at these junctions. The protein does not necessarily have to interact with components of AJs. Since the protein interacts with itself in vitro, it is possible that it forms a lattice that reaches into the apical portion of the SJs without interacting with components of AJs. However, we favor the hypothesis that a yet unknown component of AJs interacts with DLT, as the absence or overexpression of DLT causes a dramatic loss of components at AJs. Finally, in a third developmental stage, DLT defines the apical boundary of SJs. This function is best illustrated with the observation that loss of DLT almost immediately leads to the apical localization of SJ markers. Later, these markers become redistributed over the entire cell membrane. This hypothesis is butressed by the observation that the proteins are colocalized or abut each other in vivo and interact in vitro and in the two-hybrid assays. We propose that DLT prevents apical localization of NRX IV by binding to the most apical belt of NRX IV. NRX IV may be unable to interact with DLT over most of the SJs because of the presence of other proteins that are associated with NRX IV. Possible candidates that prohibit binding of DLT to NRX IV include Coracle (Baumgartner et al., 1996; Ward et al., 1998) and DLG (Woods et al., 1996). Future studies aimed at identifying other molecular components that interact with DLT prior to and after cellularization may shed light on the complex process of epithelial and neural polarization.

Experimental Procedures

Yeast Two-Hybrid Screen

A 150 bp fragment that encodes the cytoplasmic domain of NRX IV was amplified using the primers CCCGGAATTCAGGTCGCTATTTG CACCGACACAAAG, CCATGCCATGGGTCGCTATTTGCACCGACA CAAAG, and CCCGCTCGAGTGGTCGCTGTTGCGTGTCTAAGGC and cloned into pAS2-CYH2 (EcoRI-XhoI) and pACT2 (NcoI-XhoI). pAS2-CYH2-NRXCT and a 0- to 20-hr-old *Drosophila* cDNA library in pACT2 (provided by Steve Elledge) were transformed into HF7c and analyzed for β-galactosidase activity. All procedures were according to Durfee et al. (1993).

Production of Recombinant Proteins, Antibodies, and Western Analysis

The SDS-denatured full-length protein was used as an antigen to immunize rabbits, and the N-terminally truncated SDS-denatured protein was used to immunize mice. Both antisera were specific to DLT. GST-fusion constructs carrying full-length ORF containing all four PDZ domains, PDZ domains 1–2, PDZ domains 3–4, and the

cytoplasmic domain of CRB were made in pGEX-4T1 (Pharmacia). All biochemical procedures were followed as described in Bhat et al. (1996). Anti-CRB rat polyclonal antibody was raised against SDS-denatured GST-fusion protein containing the cytoplasmic 37 amino acids of CRB.

Immunohistochemistry and Confocal Microscopy

The following primary antibodies were used: polyclonal rabbit anti-DLT (1:1000; this work), polyclonal mouse anti-DLT (1:500; this work), rat polyclonal anti-CRB (1:500; this work), rabbit polyclonal anti-NRX IV (1:1000; Baumgartner et al., 1996), guinea pig polyclonal anti-DLG (1:1000, Dan Woods), rat monoclonal anti-DE-CAD (1:20, Oda et al., 1994), and mouse polyclonal anti-Armadillo (1:200; Cox et al., 1996). Fluorescent secondary antibodies were from Jackson Immunochemicals. Images were captured using a Bio-Rad MRC 1024 laser-scanning confocal microscope and processed using Adobe Photoshop.

Genomic Rescue and Generation of a *dlt* Null Allele

The genomic cosmid library was obtained from John Tamkun and used to establish transgenic lines. Genomic constructs carrying *dlt* and flanking regions were made by splicing fragments, and internal deletion in *dlt* was made by deleting an internal HindIII (300 bp) fragment to truncate DLT. P element mobilization and rescue were carried out as described in Bhat et al. (1996).

Ectopic Expression of *dlt*

P{w$^+$,hs.GAL4},P{w$^+$,UAS-dlt}/P{w$^+$, hs.GAL4},P{w$^+$,UAS-dlt} embryos were collected for 0–3 hr and aged for 4 hr at room temperature. These embryos (4–7 hr) received a heat shock for 1 hr at 37.5°C in a water bath, recovered for 3 hr, and were fixed and stained. Embryos stained with anti-NRX IV were aged for 5 hr at room temperature to allow *nrx IV* expression.

dsRNA Synthesis and Injection into Embryos

dsRNA was synthesized according to Kennerdell and Carthew (1998). The templates for ds-*dlt* RNA synthesis were made by PCR using primers containing T7 promoter sequences at their 5′ ends. The 5′ and 3′ untranslated sequences were amplified using primer sets as 5′-AAGCTGTCCCACTTAGAGCCC-3′ and 5′-GGAGCCGAA TGGGAGTGCGAG-3′, and 5′-CCCGACTGGCGGAACTAGGGT-3′ and 5′-CCGGGTCCAATAGCCCTCCGC-3′. The translated sequences were amplified using primer sets as 5′-CATCGTCCACGTGCAGGA CTC-3′ and 5′-CGGCCTGGTGGTTGGAGTAGC-3′, and 5′-GGGCTC CGATGTGGAGGTGAT-3′ and 5′-CCCTAGTTCCGCCAGTCGGGA-3′. After PCR amplification, template DNA was purified by Qiagen Gel Extraction Kit, and dsRNA was synthesized using a Transcription Kit from Boehringer Mannheim. The template DNA was destroyed by DNAse I treatment, and dsRNA was further purified by phenol/chloroform extraction followed by ethanol precipitation, and dissolved in injection buffer (Rubin and Spradling, 1982). For injection, 0- to 40-min-old embryos were dechorionated and aligned such that injection location was midway between the dorsal–ventral side approximately in the middle of the egg length under halocarbon oil. The injections were carried out with Microinjector 5242 from Eppendorf, and the injected embryos were incubated at 25°C for 3 or 6 hr and processed for immunostaining.

Acknowledgments

We thank Dan Woods, Tadashi Uemura, Tim Sliter, Jim Mason, John Tamkun, Gerry Rubin, Steve Elledge, and the Indiana Stock Center for reagents and flies. We would like to thank Ullrich Tepass, Scott Goode, Gerard Karsenty, and members of the Bellen laboratory for comments on the manuscript, and Yuchun He and Bobby Kurian for technical assistance. M. A. B. was supported by the Howard Hughes Medical Institute and a National Institutes of Health training grant to Art Beaudet, and he is a Howard Temin Fellow of the National Cancer Institute. S. I. was supported by a National Science Foundation grant to H. J. B.; K.-W. C., K.-O. C., and H. J. B. acknowledge support from the National Institutes of Health. H. J. B. is an investigator of the Howard Hughes Medical Institute.

Received November 17, 1998; revised February 19, 1999.

References

Anderson, J.M. (1996). Cell signaling: MAGUK magic. Curr. Biol. *6*, 382–384.

Balda, M.S., and Matter, K. (1998). Tight junctions. J. Cell Sci. *111*, 541–547.

Baumgartner, S., Littleton, J.T., Broadie, K., Bhat, M.A., Harbecke, R., Lengyel, J.A., Chiquet-Ehrismann, R., Prokop, A., and Bellen, H.J. (1996). A *Drosophila* neurexin is required for septate junction and blood-nerve barrier formation and function. Cell *87*, 1059–1068.

Bellen, H.J., Lu, Y., Beckstead, R., and Bhat, M.A. (1998). *neurexin IV*, *caspr* and *paranodin*—novel members of the neurexin family: encounters of axons and glia. TINS *21*, 444–449.

Bhat, M.A., Philp, A.V., Glover, D.M., and Bellen, H.J. (1996). Chromatid segregation at anaphase requires the barren product, a novel chromosome-associated protein that interacts with Topoisomerase II. Cell *87*, 1103–1114.

Brand, A.H., and Perrimon, N. (1993). Targeted gene expression as a means of altering cell fates and generating dominant phenotypes. Development *118*, 401–415.

Brown, N.H. (1993). Integrins hold *Drosophila* together. BioEssays *15*, 383–390.

Chou, T.B., and Perrimon, N. (1992). Use of a yeast site-specific recombinase to produce female germline chimeras in *Drosophila*. Genetics *131*, 643–653.

Cox, R.T., Kirkpatrick, C., and Peifer, M. (1996). Armadillo is required for adherens junction assembly, cell polarity, and morphogenesis during *Drosophila* embryogenesis. J. Cell Biol. *134*, 133–148.

Cutforth, T., and Rubin, G.M. (1994). Mutations in Hsp83 and cdc37 impair signaling by the sevenless receptor tyrosine kinase in *Drosophila*. Cell *77*, 1027–1036.

Drubin, D.G., and Nelson, W.J. (1996). Origins of cell polarity. Cell *84*, 335–344.

Durfee, T., Becherer, K., Chen, P.L., Yeh, S.H., Yang, Y., Kilburn, A.E., Lee, W.H., and Elledge, S.J. (1993). The retinoblastoma protein associates with the protein phosphatase type 1 catalytic subunit. Genes Dev. *7*, 555–569.

Fire, A., Xu, S., Montgomery, M., Kostas, S.A., Driver, S.E., and Mello, C.C. (1998). Potent and specific genetic interference by double stranded RNA in *Caenorhabditis elegans*. Nature *391*, 806–811.

Foe, V.E., Odell, G.M., and Edgar, B.A. (1993). Mitosis and morphogenesis in the *Drosophila* embryo. In The Development of *Drosophila*, M. Bate and A. Marinez-Arias, eds. (Cold Spring Harbor, NY: Cold Spring Harbor Laboratory Press), pp. 1091–1130.

Gumbiner, B.M. (1996). Cell adhesion: the molecular basis of tissue architecture and morphogenesis. Cell *84*, 345–357.

Hynes, R.O. (1996). Targeted mutations in cell adhesion genes: what have we learned from them? Dev. Biol. *180*, 402–412.

Kennerdell, J.R., and Carthew, R.W. (1998). Use of dsRNA-mediated genetic interference to demonstrate that frizzled and frizzled 2 act in the wingless pathway. Cell *95*, 1017–1026.

Lee, J.K., Coyne, R.S., Dubreuil, R.R., Goldstein, L.S., and Branton, D. (1993). Cell shape and interaction defects in alpha-spectrin mutants of *Drosophila melanogaster*. J. Cell Biol. *123*, 1797–1809.

Littleton, J.T., Bhat, M.A., and Bellen, H.J. (1997). Deciphering the function of neurexins at cellular junctions. J. Cell Biol. *137*, 793–796.

Marfatia, S.M., Lue, R.A., Branton, D., and Chishti, A.H. (1994). In vitro binding studies suggest a membrane-associated complex between erythroid p55, protein 4.1, and glycophorin C. J. Biol. Chem. *269*, 8631–8634.

Marfatia, S.M., Morais-Cabral, J.H., Kim, A.C., Byron, O., Chishti, A.H. (1997). The PDZ domain of human erythrocyte p55 mediates

its binding to the cytoplasmic carboxyl terminus of glycophorin C. Analysis of the binding interface by in vitro mutagenesis. J. Biol. Chem. *272*, 24191–24197.

Muller, H.A., and Wieschaus, E. (1996). *armadillo*, *bazooka*, and *stardust* are critical for early stages in formation of the zonula adherens and maintenance of the polarized blastoderm epithelium in *Drosophila*. J. Cell Biol. *134*, 149–163.

Oda, H, Uemura, T., Harada, Y., Iwai, Y., Takeichi, M. (1994). A *Drosophila* homolog of cadherin associated with armadillo and essential for embryonic cell-cell adhesion. Dev. Biol. *165*, 716–726.

Ponting, C.P., Phillips, C., Davies, K.E., and Blake, D.J. (1997). PDZ domains: targeting signaling molecules to sub-membranous sites. Bioessays *19*, 469–479.

Rubin, G.M., and Spradling, A.C. (1982). Genetic transformation of *Drosophila* with transposable element vectors. Science *218*, 348–353.

Salzberg, A., Prokopenko, S.N., He, Y., Tsai, P., Pal, M., Maroy, P., Glover, D.M., Deak, P., and Bellen, H.J. (1997). P-element insertion alleles of essential genes on the third chromosome of *Drosophila melanogaster*: mutations affecting embryonic PNS development. Genetics *147*, 1723–1741.

Schejter, E.D., and Wieschaus, E. (1993). Functional elements of the cytoskeleton in the early *Drosophila* embryo. Annu. Rev. Cell Biol. *9*, 67–99.

Sliter, T.J., Henrich, V.C., Tucker, R.L., and Gilbert, L.I. (1989). The genetics of the Dras3-Roughened-ecdysoneless chromosomal region (62B3-4 to 62D3-4) in *Drosophila melanogaster*: analysis of recessive lethal mutations. Genetics *123*, 327–336.

Songyang, Z., Fanning, A.S., Fu, C., Xu, J., Marfatia, S.M., Chishti, A.H., Crompton, A., Chan, A.C., Anderson, J.M., and Cantley, L.C. (1997). Recognition of unique carboxyl-terminal motifs by distinct PDZ domains. Science *275*, 73–77.

Tamkun, J.W., Deuring, R., Scott, M.P., Kissinger, M., Pattatucci, A.M., Kaufmann, T.C., and Kennison, J.A. (1992). *brahma*: a regulator of *Drosophila* homeotic genes structurally related to the yeast transcriptional activator SNF2/SWI2. Cell *68*, 561–572.

Tepass, U. (1996). CRB, a component of the apical membrane, is required for zonula adherens formation in primary epithelia of *Drosophila*. Dev. Biol. *177*, 217–225.

Tepass, U. (1997). Epithelial differentiation in *Drosophila*. BioEssays *19*, 673–682.

Tepass, U., and Hartenstein, V. (1994). The development of cellular junctions in the *Drosophila* embryo. Dev. Biol. *161*, 563–596.

Tepass, U., Theres, C., and Knust, E. (1990). *crumbs* encodes an EGF-like protein expressed on apical membranes of *Drosophila* epithelial cells and required for organization of epithelia. Cell *61*, 787–799.

Tepass, U., Gruszynski-DeFeo, E., Haag, T.A., Omatyar, L., Torok, T., and Hartenstein, V. (1996). *shotgun* encodes *Drosophila* E-cadherin and is preferentially required during cell rearrangement in the neurectoderm and other morphogenetically active epithelia. Genes Dev. *15*, 672–685.

Uemura, T., Oda, H., Kraut, R., Hayashi, S., Kataoka, Y., and Takeichi, M. (1996). Zygotic *Drosophila* E-cadherin expression is required for processes of dynamic epithelial cell rearrangement in the *Drosophila* embryo. Genes Dev. *10*, 659–671.

Wang, M., Champion, L.E., Biessmann, H., and Mason, J.M. (1994). Mapping a mutator, mu2, which increases the frequency of terminal deletions in *Drosophila melanogaster*. Mol. Gen. Genet. *245*, 598–607.

Ward, R.E., IV, Lamb, R.S., and Fehon, R.G. (1998). A conserved functional domain of *Drosophila* coracle is required for localization at the septate junction and has membrane-organizing activity. J. Cell Biol. *23*, 1463–1473.

Wodarz, A., Grawe, F., and Knust, E. (1993). CRB is involved in the control of apical protein targeting during *Drosophila* epithelial development. Mech. Dev. *44*, 175–187.

Wodarz, A., Hinz, U., Engelbert, M., and Knust, E. (1995). Expression of CRB confers apical character on plasma membrane domains of ectodermal epithelia of *Drosophila*. Cell *82*, 67–76.

Woods, D.F., and Bryant, P.J. (1991). The *discs-large* tumor suppressor gene of *Drosophila* encodes a guanylate kinase homolog localized at septate junctions. Cell *66*, 451–464.

Woods, D.F., and Bryant, P.J. (1993). ZO-1, DlgA and PSD-95SAP90: homologous proteins in tight, septate and synaptic cell junctions. Mech. Dev. *44*, 85–89.

Woods, D.F., Hough, C., Peel, D., Callaini, G., and Bryant, P.J. (1996). Dlg protein is required for junction structure, cell polarity, and proliferation control in *Drosophila* epithelia. J. Cell Biol. *134*, 1469–1482.

Yap, A.S., Brieher, W.M., and Gumbiner, B.M. (1997). Molecular and functional analysis of cadherin-based adherens junctions. Annu. Rev. Cell Dev. Biol. *13*, 119–146.

GenBank Accession Number

The accession number for the *dlt* sequence reported in this paper is AF103942.